Available online at www.sciencedirect.com

SciVerse ScienceDirect

Mathematics and Computers in Simulation 82 (2012) 909–923

MATHEMATICS AND COMPUTERS IN SIMULATION

www.elsevier.com/locate/matcom

Original article

An optimal control methodology for plant growth—Case study of a water supply problem of sunflower

Lin Wu [a,b,*], François-Xavier Le Dimet [c,d], Philippe de Reffye [e,f], Bao-Gang Hu [g], Paul-Henry Cournède [e,h], Meng-Zhen Kang [g]

[a] *Université Paris-Est, CEREA, joint laboratory Ecole des Ponts ParisTech – EDF R&D, Marne la Vallée F-77455, France*
[b] *INRIA, Clime, Rocquencourt F-78153, France*
[c] *Université Joseph Fourier, Lab. Jean Kuntzmann (LJK), Grenoble F-38041, France*
[d] *INRIA, MOISE, Grenoble F-38041, France*
[e] *INRIA, DigiPlante, Orsay F-91893, France*
[f] *CIRAD, UMR AMAP, Montpellier F-34000, France*
[g] *Chinese Academy of Sciences, Institute of Automation, LIAMA, Beijing 100080, China*
[h] *Ecole Centrale Paris, Laboratory of Applied Mathematics, Châtenay-Malabry F-92295, France*

Received 17 December 2010; received in revised form 13 November 2011; accepted 22 December 2011
Available online 18 January 2012

Abstract

An optimal control methodology is proposed for plant growth. This methodology is demonstrated by solving a water supply problem for optimal sunflower fruit filling. The functional–structural sunflower growth is described by a dynamical system given soil water conditions. Numerical solutions are obtained through an iterative optimization procedure, in which the gradients of the objective function, i.e. the sunflower fruit weight, are calculated efficiently either with adjoint modeling or by differentiation algorithms. Further improvements in sunflower yield have been found compared to those obtained using genetic algorithms in our previous studies. The optimal water supplies adapt to the fruit filling. For instance, during the mid-season growth, the supply frequency condenses and the supply amplitude peaks. By contrast, much less supplies are needed during the early and ending growth stages. The supply frequency is a determining factor, whereas the sunflower growth is less sensitive to the time and amount of one specific irrigation. These optimization results agree with common qualitative agronomic practices. Moreover they provide more precise quantitative control for sunflower growth.

Keywords: Functional–structural plant model; Dynamical system; Optimal control; Adjoint model

1. Introduction

Functional–structural plant models (FSPMs [33,34,28]) combine process-based models and architectural models for better description of plant growth. The process-based models characterize plant mechanisms like photosynthesis for agronomic applications [24,8]. By contrast, the architectural models were originally developed to analyze botanic

* Corresponding author at: Université Paris-Est, CEREA, joint laboratory Ecole des Ponts ParisTech – EDF R&D, Marne la Vallée F-77455, France.
E-mail address: Lin.Wu@cerea.enpc.fr (L. Wu).

0378-4754/$36.00 © 2012 IMACS. Published by Elsevier B.V. All rights reserved.
doi:10.1016/j.matcom.2011.12.007

patterns [14] or topological structures [32]. A typical FSPM can thus simulate not only plant organogenesis, but also biomass production and partition at organ level (leaf, internode, fruit, etc.). This leads to many FSPM applications, such as breeding and yield optimization [20,29].

Several FSPMs have been proposed, e.g. GROGRA [17], LIGNUM [27], L-systems variants [26], and GreenLab [39,7]. An interesting GreenLab characteristic is that it simulates the plant functional–structural growth by a mathematical recursive algorithm formulated as dynamical equations. This growth algorithm is based on a minimal set of physiological knowledge, such as the empirical rules of plant–environment interactions for biomass acquisition and the source–sink relations among organs that compete for assimilates. Consequently, the plant morphological plasticity can be described with a small set of endogenous parameters. The complexity of parameter calibrations is thus reduced [12]. The usability of GreenLab for practical applications has been justified by the resulting stable calibrated parameters cross phenotypic plasticity [22]. The main challenging issue of FSPMs is the balance between mathematical clarity and physiological complexity.

The mathematical transparency of GreenLab makes it natural to be formulated as a discrete dynamical system:

$$\begin{cases} \mathbf{x}(n) = F(\mathbf{x}(n-1), \boldsymbol{\Theta}, \mathbf{u}(n-1)), \\ \mathbf{x}(0) = \boldsymbol{\Upsilon}, \end{cases} \tag{1}$$

where n is the time index, F is a nonlinear operator, $\mathbf{x}$ is the state vector, $\boldsymbol{\Upsilon}$ is the initial state at time step $n=0$, $\mathbf{u}$ is the input data or control vector, and $\boldsymbol{\Theta}$ is the set of model endogenous parameters. The solution of Eq. (1) gives the trajectory of system state, with which different types of problems can be defined [38]. For example, the *calibration* problem is to find optimal $\boldsymbol{\Theta}$ to minimize the discrepancy between model simulations and experimental observations. The *state estimation* problem is to retrieve the state status by optimizing the phenotype-specific parameters such as the exogenous input data U and the initial state $\boldsymbol{\Upsilon}$. Whereas the *control* problem is to find U, sometimes also $\boldsymbol{\Theta}$ and $\boldsymbol{\Upsilon}$, to optimize a given objective or criterion, e.g. the yield. These formulations are still not well recognized in the FSPM community.

The FSPM control problem is a difficult issue because of the nonlinearity of the plant system. In many cases even discontinuity is involved. This nonlinearity is due to the biological thresholding or saturation effects. It prohibits exact analytical solutions of the control problem. Heuristic searching methods based on GreenLab have been proposed for numerical solutions [38,29]. These methods are simulation-based; the plant system is treated as a black-box model. As a result, the advantage of the mathematical transparency of GreenLab unfortunately fades out. Furthermore, they scale badly with the dimension of the control parameter space and suffer from the curse of dimensionality.

In this paper, we propose an optimal control methodology for plant functional–structural growth, in which the gradient of the objective function can be efficiently computed by adjoint modeling [21,19]. This makes it feasible to solve the plant control problem using classic descent algorithms. Contrary to the heuristic methods, this methodology scales well with the large-scale systems, e.g. those in atmospheric science of which the dimension of state vector usually goes beyond a million [30,37].

This optimal control methodology is demonstrated by solving a sunflower water supply problem. This irrigation problem has been investigated in our previous study using a genetic algorithm in which only four parameters are controlled [38]. In this study, much more exogenous control parameters will be optimized. Note that we are not aiming at an operational solution of a practical irrigation problem, but rather an evaluation of the performance of this optimal control methodology. Yet hopefully some physiological insights could be inferred by examining the resulting optimal water supplies.

The paper is organized as follows. In Section 2, each component in Eq. (1) is explicitly specified for our plant–soil dynamical system. The optimal control methodology for the sunflower water supply problem is presented in Section 3, in which is derived the adjoint model of the control system, as well as the practical calculation of gradients using differential algorithms. The solution of the optimal watering problem is given with physiological interpretation in Section 4. A general discussion as well as perspectives are given in the last section.

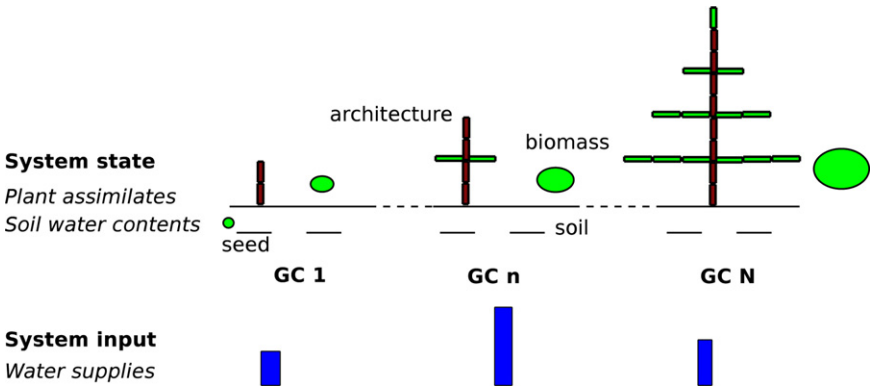

Fig. 1. Schematic of plant functional–structural growth [43] under soil water conditions.

2. Dynamics formulation

In this section, we present how plant growth can be described by discrete dynamical equations. Detailed botanic concepts and physiological knowledge can be found in [32,39]. The soil moisture model and its interaction with plant are treated in the same way as in [38].

2.1. Functional–structural plant growth in interaction with soil water conditions

We formulate plant growth at organ level. The functional–structural growth is sketched in Fig. 1. Plant is assumed to undergo Growth Cycles (GCs) of a biological clock. During each GC the plant metabolism results in the emergence of a cohort of new organs. The GC can vary from several days (cottons) to one year (trees of temperate regions). However, the sum of the daily temperatures during the GC is assumed to be quite constant [31].

At every GC, the plant produces biomass by leaf photosynthesis. If the microclimatic environment conditions around each leaf are identical, then $Q(n)$, the biomass produced by the photosynthesis of all the leaves during GC n, can be calculated by an empirical nonlinear function Ψ with respect to the environmental conditions, the number of leaves, the leaf surface areas, and some hidden parameters. In [39], the nonlinear function is chosen as

$$Q(n) = \Psi(S, E, r1, r2) = \sum_{a=1}^{n} \left(N_l(a, n) \cdot \frac{E(n)}{(r_1/S(a, n)) + r_2} \right), \tag{2}$$

where $N_l(a, n)$ is the number of leaves of Chronological Age a (CA, counted by GCs) at GC n, $S(a, n)$ is their surface area, $r1$, $r2$ are hidden parameters to be assessed, $E(n)$ is the average biomass production potential depending on environmental conditions, such as light, temperature and soil water content.

For each organ, we define its demand as its ability to attract biomass. The organ demand d_o depends on organ CA j and organ type o ($o = l, e, c, f, m$ refers respectively to leaf, internode, layer, female flower and male flower), and is calculated as

$$d_o(j) = P_o \phi_o(j), \tag{3}$$

where P_o are the organ sink strengths, ϕ_o are normalized distribution functions characterizing the evolution of the sink strengths from CA 1 to CA t_o with t_o being the organ lifespan. In this study, ϕ_os are chosen to be beta functions with hidden function parameters. The total biomass demand of all plant organs at GC n is as

$$D(n) = \sum_{o} \sum_{a=1}^{t_o} N_o(a, n) \cdot d_o(a), \tag{4}$$

where $N_o(a, n)$ is the number of o-type organs of CA a at GC n. The organ numbers can be calculated by automaton [39] or botanic growth grammar [36, Ch. 2].

The biomass produced by photosynthesis is redistributed among all organs according to the ratio between their demands d_o with respect to total plant demand $D(n)$. This instantaneously leads to the calculation of the biomass increment $\Delta q_o(a, n)$ and total cumulated biomass $q_o(a, n)$ for any o-type organ of CA a at the current GC n:

$$\begin{aligned}\Delta q_o(a,n) &= \frac{d_o(a)}{D(n)} \cdot Q(n-1),\\ q_o(a,n) &= \sum_{j=1}^{a} \Delta q_o(j, n-(a-j)) = P_o \sum_{j=1}^{a} \frac{\phi_o(j) \cdot Q(n-(a-j)-1)}{D(n-(a-j))}.\end{aligned} \tag{5}$$

Given plant geometry configurations (organ shape and size, phyllotaxy), we can thus construct 3D plants through Eq. (5).

The biomass production potential E during GC n is supposed to be linearly proportional to the current soil water content. The light, temperature, and mineral conditions are assumed to be optimal and the plant suffers from no stress (for a complete formula, see [36]):

$$E(n) = \begin{cases} 0 & Q_w(n) \le Q_{wmn}, \\ \kappa \cdot \dfrac{Q_w(n) - Q_{wmn}}{\beta(Q_{wmx} - Q_{wmn})} & Q_{wmn} < Q_w(n) \le (1-\beta)Q_{wmn} + \beta Q_{wmx}, \\ \kappa & Q_w(n) > (1-\beta)Q_{wmn} + \beta Q_{wmx}, \end{cases} \tag{6}$$

where $Q_w(n)$ is the soil water content at GC n, Q_{wmn} corresponds to the wilt point of soil water content beneath which the plant cannot extract water from soil, Q_{wmx} is the water field capacity above which the water flows away, and κ is an empirical parameter. Plant suffers from water stress when $(Q_w(n) - Q_{wmn})/(Q_{wmx} - Q_{wmn}) < \beta$ with $\beta = 0.4$. The thresholds here make the system strongly nonconvex. The biomass production potential formula Eq. (6) is a simplified account of the plant–soil system for the test of our optimal control methodology. More complex descriptions are possible. For instance, precise extinction law could be employed based on adjusted leaf area index (LAI) to account for plant populational products [12], and realistic water stress model could also be introduced [23]. However, mathematically it does not change much the underlying optimal control problem.

Plants participate in soil water circulation by transpiration. Water is taken from soil by roots and flows through the plant hydraulic network up to the leaves, where water is transpired to provide necessary energy fluxes for photosynthesis. The water content in the superior soil layers, named soil moisture, is important for the study of bio-geophysical processes in agricultural or forestry ecosystems. Soil water balance is achieved when we simplify this complex soil–plant system by concentrating on plant transpiration, soil evapotranspiration, and water supply from both irrigation and precipitations. The soil water content in soil per surface unit (Q_w) is calculated by the difference equation [38]:

$$Q_w(n) - Q_w(n-1) = \underbrace{-c_1(Q_w(n-1) - Q_{wmn})}_{\text{soil evapotranspiration}} + \underbrace{c_2(Q_{wmx} - Q_w(n-1))U(n-1)}_{\text{water absorption}} - \underbrace{\rho \cdot Q(n-1)}_{\text{plant transpiration}}, \tag{7}$$

where $U(n-1)$ (a scalar) is the water supply during GC $n-1$, c_1 is an evapotranspiration coefficient, and c_2 is an absorption coefficient. The plant transpiration is assumed to be linearly proportional to biomass production [15], and ρ is the ratio between plant transpiration and plant biomass production during GC $n-1$.

2.2. Dynamical system

Supposing constant mass per unit area ϵ, the leaf surface area $S(a, n)$ can be calculated by dividing leaf mass $q_l(a, n)$ by ϵ. Substituting $S(a, n)$ into Eq. (2), we have a recursive equation for the total biomass produced at GC n without explicitly calculating the geometrical sizes of the leaves [39]:

$$Q(n) = E(n) \cdot \sum_{a=1}^{t_w} \frac{N_l(a,n) \cdot \sum_{j=1}^{a} \frac{\phi_l(j) \cdot Q(n-(a-j)-1)}{D(n-(a-j))}}{A + B \cdot \sum_{j=1}^{a} \frac{\phi_l(j) \cdot Q(n-(a-j)-1)}{D(n-(a-j))}}. \tag{8}$$

Here $A = r_1\epsilon/P_l$, $B = r_2$, and t_w is the leaf functioning period for photosynthesis. Let $\mathbf{x}(n-1)$, $\mathbf{x}(n)$ be the state vector at GC $n-1$ and n respectively:

$$\mathbf{x}(n-1) = \begin{bmatrix} Q(n-t_w) \\ \vdots \\ Q(n-2) \\ Q(n-1) \\ Q_w(n-1) \end{bmatrix}, \qquad \mathbf{x}(n) = \begin{bmatrix} Q(n-t_w+1) \\ \vdots \\ Q(n-1) \\ Q(n) \\ Q_w(n) \end{bmatrix}.$$

we can then rewrite the soil–plant system (6)–(8) in one difference equation:

$$\begin{cases} \mathbf{x}^j(n) = \mathbf{x}^{j+1}(n-1), \quad j = 1, \ldots, t_w - 1, \\ \mathbf{x}^{t_w}(n) = \kappa \cdot \dfrac{\mathbf{x}^{t_w+1}(n) - Q_{wmn}}{\beta(Q_{wmx} - Q_{wmn})} \displaystyle\sum_{a=1}^{t_w} \frac{N_l(a,n) \cdot \sum_{j=1}^{a} \dfrac{\phi_l(j) \cdot \mathbf{x}^{t_w-a+j}(n-1)}{D(n-(a-j))}}{A + B \cdot \sum_{j=1}^{a} \dfrac{\phi_l(j) \cdot \mathbf{x}^{t_w-a+j}(n-1)}{D(n-(a-j))}}, \\ \mathbf{x}^{t_w+1}(n) = (1 - c_1 - c_2 \cdot U(n-1))\mathbf{x}^{t_w+1}(n-1) + Q_{wmn}c_1 + Q_{wmx}c_2 \cdot U(n-1) - \rho \cdot \mathbf{x}^{t_w}(n-1), \end{cases} \tag{9}$$

where the superscripts of $\mathbf{x}$ denote the index of its components, the control vector $U(n-1)$ is the water supply at GC $n-1$. The endogenous parameter set $\boldsymbol{\Theta}$ is composed of hidden parameters r_1, r_2, P_o, ϕ_o and soil moisture parameters c_1, c_2. Note that in system (9), only P_l and ϕ_l are used. However, P_o and ϕ_o are also needed to compute the biomass of o-type organ. The initial condition is

$$\mathbf{x}(0) = \boldsymbol{\Upsilon} = \begin{bmatrix} 0 \\ \vdots \\ 0 \\ Q_0 \\ Q_{w0} \end{bmatrix}, \tag{10}$$

where Q_0 is seed biomass, and Q_{w0} is the initial soil water content. This completes the detailed formulation of dynamical system Eq. (1) for our water supply problem.

3. Optimal control methodology

3.1. An optimal control problem for sunflower water supply

The sunflower water supply problem is to find optimal irrigation strategies for maximal fruit production under limited water resource conditions. We chose a 63 GC sunflower growth. The hidden parameters in $\boldsymbol{\Theta}$ are set according to calibration results [40,13]. The soil moisture parameters c_1, c_2 are set to empirical values from previous studies.

Substituting the biomass production Q by the corresponding component of state vector $\mathbf{x}$, we rewrite the fruit accumulated biomass Eq. (5) as follows:

$$q_f(t_f, N) = \sum_{j=1}^{t_f} \Delta q_f(j, N) = P_f \sum_{j=1}^{t_f} \frac{\phi_f(j) \cdot \mathbf{x}^{t_w}(N - (t_f - j) - 1)}{D(N - (t_f - j))}, \tag{11}$$

where N is the number of total sunflower growth GCs, and t_f is the fruit CA. In the sunflower simulation, $N = 63$ GC, and fruit appears at 38 GC thus $t_f = 63 - 38 = 25$ GC.

For convenience, hereafter the GC numbers are moved to subscript of the vectors, e.g. $\mathbf{x}_n$ for $\mathbf{x}(n)$. If we define a function l as

$$\begin{cases} l(\mathbf{x}_n, U_n) = \Delta q_f(N-n, N), & n \geq N - t_f, \\ l(\mathbf{x}_n, U_n) = 0, & n < N - t_f, \end{cases} \tag{12}$$

then the final fruit biomass production can be formulated as a function:

$$\mathcal{J}(\mathbf{U}) = q_f(t_f, N) = \sum_{n=0}^{N-1} l(\mathbf{x}_n, U_n), \tag{13}$$

where $\mathbf{U} = [U_0, \ldots, U_{N-1}]^{\mathrm{T}} \in \mathbb{R}^N$ is the water supply vector of 63 dimension for all GCs. Here T denotes the transpose of a vector or a matrix. The maximal fruit biomass production with respect to water supply $\mathbf{U}$ is the solution of the following optimal control system:

$$\begin{cases} \begin{cases} \mathbf{x}_n = F(\mathbf{x}_{n-1}, \boldsymbol{\Theta}, U_{n-1}), \\ \mathbf{x}_0 = \boldsymbol{\Upsilon}, \end{cases} \\ \underset{\mathbf{U}\in\mathbb{R}^N}{\operatorname{argmax}}\, \mathcal{J}(\mathbf{U}), \end{cases} \tag{14}$$

where F is a vector function of $(t_w + 1)$ dimension. In numerous cases, water resources are limited due to drought or economic reasons. We thus suppose the water supplies are under the following constraints,

$$\begin{cases} \sum_{i=0}^{N-1} U_i \leq \Pi, \\ U_i \geq 0, \end{cases} \quad i = 0, \ldots, N-1, \tag{15}$$

where Π is a given total quantity of water supply during the sunflower growth.

3.2. Descent algorithms

The numerical solution of the optimal control problem Eq. (14) can be obtained by descent algorithms, in which a series of points $\{\mathbf{U}^k, k = 0, 1, 2, \ldots\}$ can be constructed by

$$\mathbf{U}^{k+1} = \mathbf{U}^k + \alpha^k \mathbf{d}^k, \tag{16}$$

where $\mathbf{d}^k$ is the direction along which $\mathbf{U}^{k+1}$ a better objective function value than $\mathbf{U}^k$ can be found. The iteration step α^k can be determined by the following unidimensional optimization problem,

$$\alpha^k = \underset{\alpha}{\operatorname{argmax}}\, \mathcal{J}(\mathbf{U}^k + \alpha \mathbf{d}^k) \tag{17}$$

The maximization problem can be converted into a minimization problem by simply inverting the sign of $\mathcal{J}$. In this case $\mathbf{d}^k$ is a descent direction. A popular choice of $\mathbf{d}^k$ is the steepest descent direction which is the negative gradient of the objective function. More complicated choices are possible, e.g. the quasi-Newton methods [3]. Most efficient optimization methods are based on gradients [10]. In this study, a descent algorithm, the sequential quadratic programming (SQP) [2], in which quadratic subproblems are constructed, is used to solve our constrained optimization problem. The iterations stop when directional derivatives along searching direction $\mathbf{d}^k$ tend to zero. It is important to note that, because of the high nonconvexity of the plant model, the convergence of the descent methods is not guaranteed, and the solutions can be local optima.

3.3. Adjoint model for gradient calculations

The optimal control methodology provides efficient techniques to compute the gradients of the objective function by introducing the adjoint model of the original dynamical model [21,19].

Suppose that U_n, $\mathbf{x}_n$ are p-dimensional and m-dimensional vectors respectively. For our water supply problem, $p=1$ and $m = t_w + 1$. The first-order variations in the state vector $\mathbf{x}$ and the objective function $\mathcal{J}$ resulting from a perturbation $\widehat{\mathbf{U}}$ on the control vector $\mathbf{U}$, denoted as $\widehat{\mathbf{x}}$ and $\widehat{\mathcal{J}}$, can be derived as follows

$$\begin{cases} \widehat{\mathbf{x}}_{n+1} = \dfrac{\partial F}{\partial \mathbf{x}}(\mathbf{x}_n, U_n)\widehat{\mathbf{x}}_n + \dfrac{\partial F}{\partial U}(\mathbf{x}_n, U_n)\widehat{U}_n, \\ \widehat{\mathbf{x}}_0 = 0, \end{cases} \tag{18}$$

$$\widehat{\mathcal{J}} = \sum_{n=0}^{N-1}\left(\frac{\partial l}{\partial \mathbf{x}}(\mathbf{x}_n, U_n)\widehat{\mathbf{x}}_n + \frac{\partial l}{\partial U}(\mathbf{x}_n, U_n)\widehat{U}_n\right) = \sum_{n=0}^{N-1}\left(\frac{\partial l}{\partial \mathbf{x}}(\mathbf{x}_n, U_n)\widehat{\mathbf{x}}_n\right) + \sum_{n=0}^{N-1}\left(\frac{\partial l}{\partial U}(\mathbf{x}_n, U_n)\widehat{U}_n\right). \tag{19}$$

Eq. (18) is the so-called *tangent linear model*. Let $\mathbb{M}^{i\times j}$ denote the set of matrices with i rows and j columns, we have

$$\frac{\partial F}{\partial \mathbf{x}} = [a_{ij}]_{m\times m} \in \mathbb{M}^{m\times m},\ \widehat{\mathbf{x}}_n \in \mathbb{M}^{m\times 1}; \qquad \frac{\partial F}{\partial U} \in \mathbb{M}^{m\times p},\ \widehat{U}_n \in M^{p\times 1}; \quad \frac{\partial l}{\partial \mathbf{x}} \in \mathbb{M}^{1\times m},\ \frac{\partial l}{\partial U} \in \mathbb{M}^{1\times p}.$$

Here each component a_{ij} of the Jacobian matrix $\partial F/\partial \mathbf{x}$ is a partial derivative of ith function of F with respect to jth component of state vector $\mathbf{x}$.

If we define a vector of adjoint variables $\overline{\mathbf{x}}_n$ that are governed by the following *adjoint model*

$$\begin{cases} \overline{\mathbf{x}}_n = \left[\dfrac{\partial F}{\partial \mathbf{x}}(\mathbf{x}_n, U_n)\right]^{\mathrm{T}}\overline{\mathbf{x}}_{n+1} + \left[\dfrac{\partial l}{\partial \mathbf{x}}(\mathbf{x}_n, U_n)\right]^{\mathrm{T}}, \quad n = N-1, \ldots, 0, \\ \overline{\mathbf{x}}_N = 0, \end{cases} \tag{20}$$

then the gradient $\nabla\mathcal{J}$ with respect to $\mathbf{U}$ can be calculated as

$$\nabla\mathcal{J} = \begin{bmatrix} \left[\dfrac{\partial F}{\partial U}(\mathbf{x}_0, U_0)\right]^{\mathrm{T}}\overline{\mathbf{x}}_1 + \left[\dfrac{\partial l}{\partial U}(\mathbf{x}_0, U_0)\right]^{\mathrm{T}} \\ \vdots \\ \left[\dfrac{\partial F}{\partial U}(\mathbf{x}_{N-1}, U_{N-1})\right]^{\mathrm{T}}\overline{\mathbf{x}}_N + \left[\dfrac{\partial l}{\partial U}(\mathbf{x}_{N-1}, U_{N-1})\right]^{\mathrm{T}} \end{bmatrix}. \tag{21}$$

The detailed derivation of the gradient formula (21) is presented in Appendix A. This gradient formula is for the general case, in which the function l in system (14) depends on both $\mathbf{x}_n$ and U_n. For our specific case, the function l in Eq. (12) does not depend on U explicitly, therefore $\partial l/\partial U$ equals zero. Note that the adjoint variable $\overline{\mathbf{x}}$ is zero at $n=N$: $\overline{\mathbf{x}}_N = 0$. Consequently the gradient formula becomes:

$$\nabla\mathcal{J} = \begin{bmatrix} \left[\dfrac{\partial F}{\partial U}(\mathbf{x}_0, U_0)\right]^{\mathrm{T}}\overline{\mathbf{x}}_1 \\ \vdots \\ \left[\dfrac{\partial F}{\partial U}(\mathbf{x}_{N-2}, U_{N-2})\right]^{\mathrm{T}}\overline{\mathbf{x}}_{N-1} \\ 0 \end{bmatrix}. \tag{22}$$

The *optimality system* is defined as the aggregation of the dynamical model and objective function (14), the adjoint model (20), and the gradient formula (21) (see [18] for more discussions on the optimality system).

3.4. Differentiation algorithm to generate the adjoint code for gradient calculations

The main difficulty is to implement the adjoint model. In most cases, the derivation of the adjoint model and its implementation, as presented in the previous section, are time-consuming and error-prone especially for complex dynamical models. Nowadays, almost all the complex models are implemented as computer programs. An alternative

approach is to obtain directly the code of adjoint models based on the code of original dynamical models. This can be carried out either following some coding conventions [35] or using an automatic differentiation software [11].

Now we show how a systematic approach can be conducted to obtain the *adjoint code* for our water supply problem. Let

$$J_n = \sum_{i=0}^{n-1} l(\mathbf{x}_i, U_i), \tag{23}$$

and let $\mathbf{X}_n = [\mathbf{U}, \mathbf{x}_n, J_n]^{\mathrm{T}}$ be the augmented state vector of $N+m+1$ dimension, we have the following dynamical system:

$$\mathbf{X}_n = M_n(\mathbf{X}_{n-1}), \quad n = 1, \ldots, N, \tag{24}$$

where M_n is the function that maps $\mathbf{X}_{n-1}$ to $\mathbf{X}_n$ according to the plant dynamics Eq. (14) and the fruit accumulation Eq. (23). The initial condition of this system is: $\mathbf{X}_0 = [\mathbf{U}, \mathbf{x}_0, J_0]^{\mathrm{T}}$.

Applying (24) from GC 1 to N successively, we get

$$\mathbf{X}_N = M_N(M_{N-1}(\cdots M_1(\mathbf{X}_0)\cdots)). \tag{25}$$

Perturbing $\mathbf{U}$ by $\widehat{\mathbf{U}}$, the tangent linear model of direct model (24) can be obtained:

$$\widehat{\mathbf{X}}_n = \mathbf{A}_n \widehat{\mathbf{X}}_{n-1}, \quad n = 1, \ldots, N, \tag{26}$$

where $\mathbf{A}_n$ is the linearized form of M_n. Denoting $\mathbf{P} = [\mathbf{I}_N\, \mathbf{0}]^{\mathrm{T}} \in \mathbb{M}^{(N+m+1)\times N}$, where $\mathbf{0}$ is zero matrix, and $\mathbf{I}_N$ stands for N-by-N identity matrix, we have $\widehat{\mathbf{X}}_0 = \mathbf{P}\widehat{\mathbf{U}}$. Repeatedly applying tangent linear model (26) from GC 1 to N leads to:

$$\widehat{\mathbf{X}}_N = \mathbf{A}_N \mathbf{A}_{N-1} \cdots \mathbf{A}_1 \mathbf{P} \widehat{\mathbf{U}}. \tag{27}$$

Denote $\mathbf{Q} = [\mathbf{0}\ 1] \in \mathbb{M}^{1\times(N+m+1)}$, and note that $\mathcal{J} = J_N$, we have:

$$\widehat{\mathcal{J}} = \mathbf{Q}\widehat{\mathbf{X}}_N = \langle \mathbf{Q}^{\mathrm{T}}, \widehat{\mathbf{X}}_N \rangle_{\mathbb{R}^{N+m+1}}, \tag{28}$$

where $\langle\rangle_{\mathbb{R}^{N+m+1}}$ is the inner product in Euclidean space $\mathbb{R}^{N+m+1}$.

Let us define the adjoint operator A^* of a linear operator A by

$$\langle x, Ay \rangle_{\mathcal{E}} = \langle A^* x, y \rangle_{\mathcal{F}}, \tag{29}$$

where $x \in \mathcal{E}$, $y \in \mathcal{F}$. Here $\mathcal{E}, \mathcal{F}$ are Euclidean spaces equipped with inner products $\langle\,\rangle_{\mathcal{E}}$, $\langle\,\rangle_{\mathcal{F}}$. The linear operator in this case usually takes the form of a matrix, and the adjoint operator A^* is simply the transpose of matrix A.

Substitute (27) into (28) and apply the definition of adjoint operator, we have

$$\widehat{\mathcal{J}} = \langle \mathbf{Q}^{\mathrm{T}}, \widehat{\mathbf{X}}_N \rangle_{\mathbb{R}^{N+m+1}} = \langle \mathbf{Q}^{\mathrm{T}}, \mathbf{A}_N \mathbf{A}_{N-1} \cdots \mathbf{A}_1 \mathbf{P} \widehat{\mathbf{U}} \rangle_{\mathbb{R}^{N+m+1}} = \langle \mathbf{P}^{\mathrm{T}} \mathbf{A}_1^{\mathrm{T}} \cdots \mathbf{A}_{N-1}^{\mathrm{T}} \mathbf{A}_N^{\mathrm{T}} \mathbf{Q}^{\mathrm{T}}, \widehat{\mathbf{U}} \rangle_{\mathbb{R}^N}. \tag{30}$$

Note that $\widehat{\mathcal{J}} = \langle \nabla \mathcal{J}, \widehat{\mathbf{U}} \rangle_{\mathbb{R}^N}$, one obtains

$$\nabla \mathcal{J} = \mathbf{P}^{\mathrm{T}} \mathbf{A}_1^{\mathrm{T}} \cdots \mathbf{A}_{N-1}^{\mathrm{T}} \mathbf{A}_N^{\mathrm{T}} \mathbf{Q}^{\mathrm{T}} \tag{31}$$

If we define an adjoint model:

$$\begin{cases} \overline{\mathbf{X}}_{n-1} = \mathbf{A}_n^{\mathrm{T}} \overline{\mathbf{X}}_n, \\ \overline{\mathbf{X}}_N = \mathbf{Q}^{\mathrm{T}}, \end{cases} \quad n = N, \ldots, 1, \tag{32}$$

a backward integration of adjoint model (32) from GC N to 1 provides the gradient:

$$\nabla \mathcal{J} = \mathbf{P}^{\mathrm{T}} \overline{\mathbf{X}}_0 = \overline{\mathbf{U}}. \tag{33}$$

In practice, the linear operator $\mathbf{A}_i$ is implemented by lines of computer code, which are a series of elementary statements of linear operations. Each statement can be considered as an elementary matrix imposed on intermediate variables, that is $\mathbf{A}_i = \mathbf{A}_i^1 \mathbf{A}_i^2 \cdots$. The transpose of $\mathbf{A}_i$ is $\cdots \mathbf{A}_i^{2,\mathrm{T}} \mathbf{A}_i^{1,\mathrm{T}}$. The adjoint code can thus be generated systematically as follows: (i) set the control variable (in our case the water supply vector $\mathbf{U}$); (ii) carry out and differentiate the

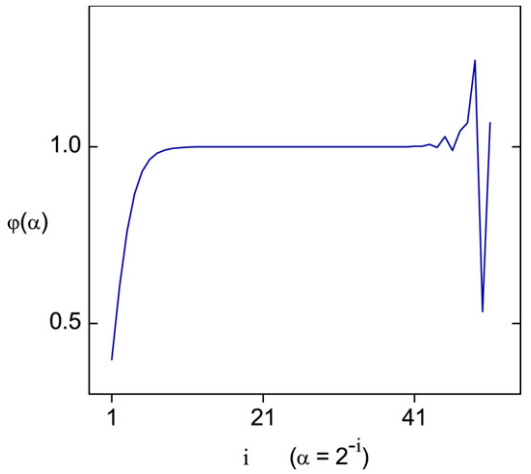

Fig. 2. Curve of the gradient validation function $\varphi(\alpha)$ with a random perturbation direction $\mathbf{h}$. For α ranging from 2^{-19} to $2^{-42}(\approx[10^{-6}, 10^{-13}])$, $\varphi(\alpha)$ approaches to 1 with errors within 10^{-4}. For large α values (left of the curve), we have truncation errors since the perturbation $\alpha\mathbf{h}$ is not significantly small compared with $\mathbf{U}$. For extremely small α values (right of the curve), the oscillation arises due to the floating-point roundoff errors.

direct code with respect to control variables with safeguards of intermediate variables that depend on control variables; (iii) associate these intermediate variables with adjoint variables; (iv) calculate these adjoint variables in a reverse manner starting from the end of the direct code by transposing differentiated (linearized) elementary statements. According to the gradient formula (33), the final value of adjoint variable $\overline{\mathbf{U}}$ equals to the gradient of the objective function $\mathcal{J}$.

We have derived the adjoint code line-by-line from the original GreenLab code (a simplified version that implements the recursive algorithm (8)). More details can be found in [36, Ch. 4]. We also refer to [42,9] on practical adjoint coding.

4. Results

4.1. Validation of gradient calculations

Consider the Taylor expansion of $\mathcal{J}(\mathbf{U})$,

$$\mathcal{J}(\mathbf{U}+\alpha\mathbf{h}) = \mathcal{J}(\mathbf{U}) + \alpha\langle\nabla\mathcal{J}, \mathbf{h}\rangle + o(\alpha|\mathbf{h}|) \tag{34}$$

where $\mathbf{h}$ is the direction of perturbations. We can check the function

$$\varphi(\alpha) = \frac{\mathcal{J}(\mathbf{U}+\alpha\mathbf{h}) - \mathcal{J}(\mathbf{U})}{\alpha\langle\nabla\mathcal{J}, \mathbf{h}\rangle} \tag{35}$$

for gradient validation [5]. This function essentially compares the gradient $\nabla\mathcal{J}$ (calculated using either adjoint model or adjoint code) with the approximate gradient obtained using finite difference. When $\alpha \to 0$, according to Taylor expansion Eq. (34), $\varphi(\alpha)$ tends to 1 for the correct gradient. We randomly choose $\mathbf{h}$, and vary α from 2^0 to 2^{-50}. Then we plot in Fig. 2 the curve of $\varphi(\alpha)$ with $\nabla\mathcal{J}$ set to the gradient obtained using adjoint code. One observes that $\varphi(\alpha)$ approaches to 1 perfectly, therefore the correctness of our adjoint code for gradient calculations can be assumed.

The gradient obtained using the adjoint model (20), in which the Jacobian matrices are approximated using finite difference, has negligible difference compared with that obtained using the adjoint code. The two approaches are also computationally comparable (adjoint code is faster). Therefore, we report only the optimization results using the adjoint code for gradient calculations.

4.2. Optimal water supplies and physiological discussions

The optimization is performed for three random initial water supplies. The corresponding iterations of the SQP descent algorithm are shown in Fig. 3 and 4. For all the three cases, the objective function values seem to converge to local optima, and the directional derivatives tend to be zero.

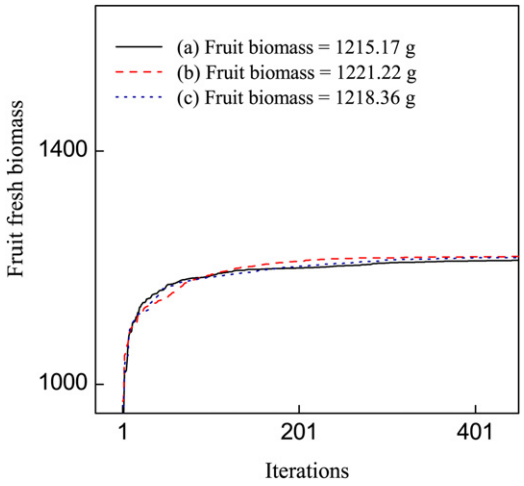

Fig. 3. Sunflower fruit biomass with respect to iteration number during optimization for three random initial water supply strategies (a–c). There are very slight differences of the objective function values after 400 iterations.

The optimal water supplies resulting from the three different initial water supplies are plotted in Fig. 5. All the three optimal supplies demonstrate a similar irrigation pattern. For the early growth stage from beginning to approximately GC 15–20, the irrigation frequency and amplitude are very low but with a tendency of densification as sunflower grows. Much more water is needed for mid-season growth, especially after fruit appears at GC 38, during which presents a rough irrigation frequency of two GCs. This growth period is characterized by prominent evapotranspiration, and the corresponding optimal water supplies peak. For the end of growth after GC 58, all the optimal supply strategies indicate that there is no need of irrigation. It seems that the irrigation frequency is the determining factor, whereas the sunflower growth is less sensitive to the time and amount of one specific irrigation. Indeed, the maximal difference in fruit biomass weight under the three optimal water supplies is 9 g, which is rather small, but the irrigation amount for a given GC could differ drastically for these optimal supply strategies. The optimal water supply strategies above are compatible with common agronomic practices [4]. Moreover, they provide precise quantitative control for sunflower growth.

In our previous study [38], we formulated this sunflower water supply problem as a mixed integer nonlinear programming problem (MINLP). A heuristic method using genetic algorithm was adapted to solve that MINLP problem. However, there were only four controlled parameters, namely two continuous parameters on the form of

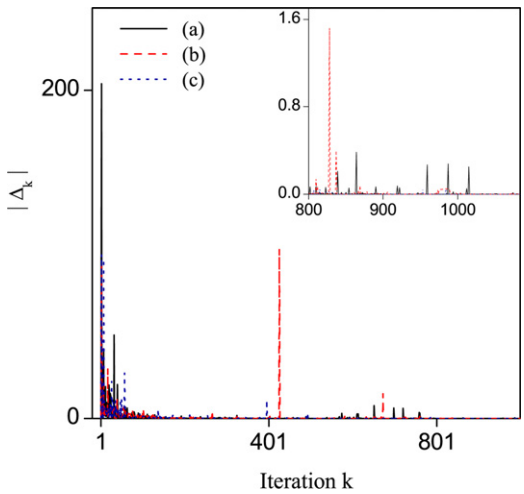

Fig. 4. Directional derivatives Δ_k with respect to iteration number (k) during optimization for three random initial water supply strategies (a–c). Here $|\Delta_k| = |\nabla \mathcal{J}(\mathbf{U}^k)^{\mathrm{T}} \mathbf{d}^k|$, where $\mathbf{U}^k$, $\mathbf{d}^k$ are the water supplies and the searching direction at iteration k.

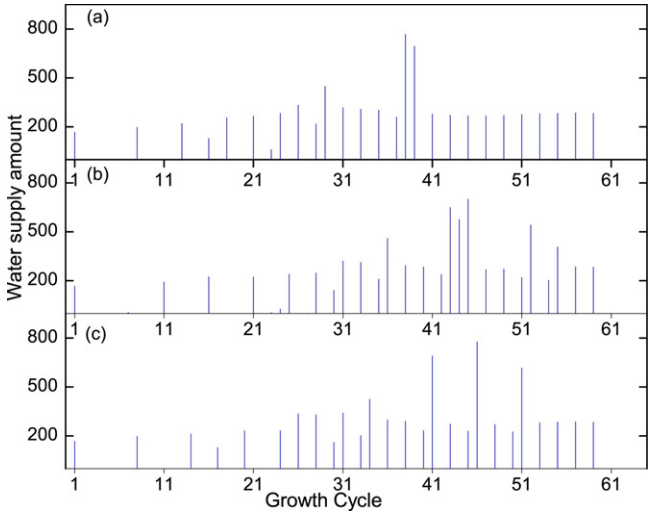

Fig. 5. Optimal water supply strategies obtained by solving the optimal control system with three random initial water supply strategies.

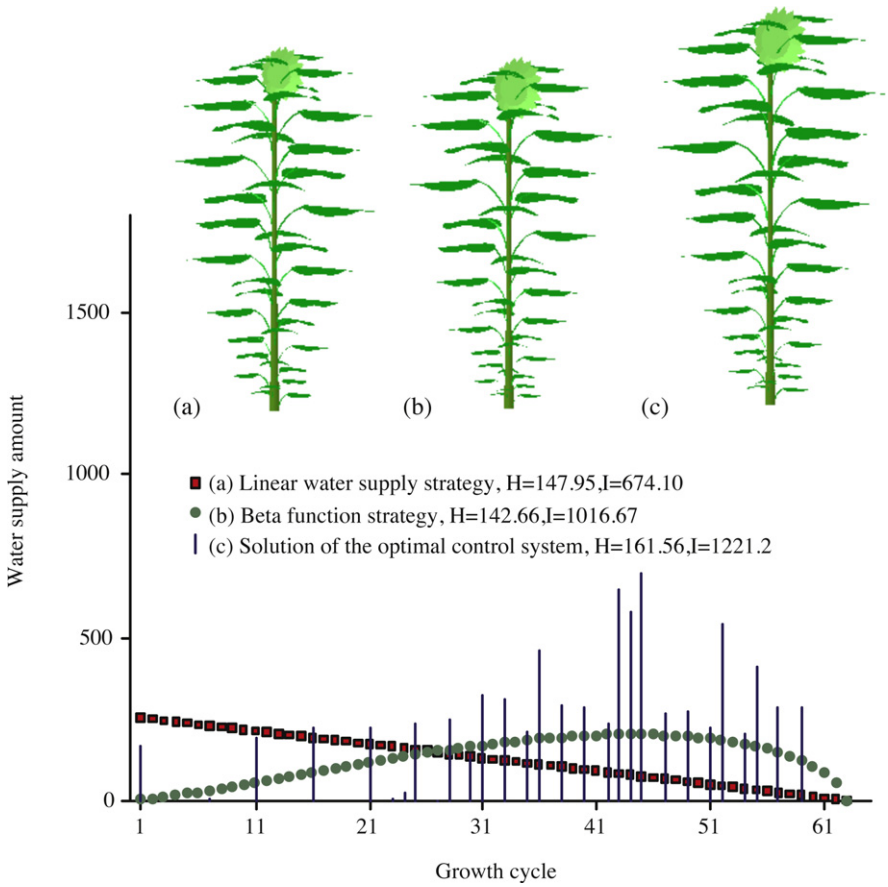

Fig. 6. Different water supply strategies and their resulting sunflower growths. Strategy (a) is linear. Strategy (b) follows a regular curve of beta function. Strategy (c) is the optimal water supply obtained using the optimal control methodology (Fig. 5b). The sunflower height is denoted by H, and fruit biomass weight by I.

supply distribution and two discrete parameters on supply frequency. The searching space was thus limited. In this paper, thanks to the optimal control methodology, totally 63 parameters, that is, water supplies for all GCs, can be optimized. This new searching space thus includes arbitrary form of water supply distribution. In addition, no global frequency is imposed for optimization. The new optimal supplies in this paper show much richer patterns adapted to the growth stages of sunflower. A relative gain of 2% in fruit biomass weight can be obtained for the new optimal water supplies compared to the previous optimal supplies reported in [38].

For comparison purpose, in Fig. 6 we plot a linear supply strategy, a regular supply strategy, and the best optimal supply strategy, as well as their resulting 3D sunflower growths. The sunflower under the regular strategy is shorter, but with a much heavier fruit, than that under the linear strategy. In the latter one, the abundance of water supply at the early growth stages favors the internode growth, and the absence of water supply at mid-season growth penalizes fruit biomass accumulation. The optimal strategy best adapts to the sunflower growth and outperforms others in both fruit weight and sunflower height. Its fruit is 20% heavier, and its height is 13% higher than those under the regular strategy. This crucial difference again indicates that the irrigation frequency plays an important role, since the optimal strategy and the regular strategy are rather qualitatively comparable. Both conduct dominant irrigations during mid-season growth and light irrigations for the early and ending growth stages.

5. Conclusion

An optimal control methodology has been introduced for the plant functional–structural growth. This methodology has been assessed by solving a sunflower water supply problem. The adjoint model and its practical implementation using differential algorithms have been developed for efficient calculation of gradients. It has been shown that this methodology scales well to control all the water supplies (totally 63 parameters) during the sunflower growth.

It has been found that the irrigation frequency and total supply amount for different growth stages are important for fruit filling. For the resulting optimal supply strategies, the supply frequency condenses and the supply amplitude peaks during the mid-season growth, when fruit appears (at 38 GC) and the optimal water conditions favor the fruit biomass accumulation. By contrast, much less water is needed during the early and ending growth stages. The sunflower growth has been found to be less sensitive to the time and amount of one specific irrigation. These findings are compatible with agronomic practices. Moreover they provide more precise quantitative control of sunflower growth.

This optimal control methodology scales well with the dimension and the complexity of underlying dynamical systems. This has been experienced in atmospheric science [30,37]. Theoretically speaking, this methodology can be extended for increasingly complex FSPMs without additional difficulties. The adjoint model or the adjoint code need to be revised accordingly, but the procedure remains the same as that in this paper. Desirable developments considering the new FSPM features are, for example, more realistic photosynthesis formula for biomass production [12], microclimate considerations at organ level [6], and interactions between architecture and functioning [25]. The optimization under uncertainties [16] would be a difficult issue related to stochastic optimal control. Further in-depth investigations are needed to apply this methodology in the real practice for operational irrigation instructions.

We have demonstrated that our optimal control methodology is effective in solving the control problems for plant growth. This methodology can also be applied to the parameter calibration and the state estimation problems. One may regret that only numerical solutions are obtained for our sunflower water supply problem. Analytical solutions are absent; rigorous analyses, e.g. the existence and uniqueness of the solution, have not been attacked. However, most of the practical complex control systems in biology and engineering bear no analytical solutions. Indeed, further investigations are needed when dealing with discontinuity [41,1] or if one wants to escape from local optima. Regularization methods may be resorted to for the latter case.

Acknowledgments

The authors would like to thank the reviewers for their thorough and detailed suggestions that helped to significantly improve the manuscript. This work is supported in part by LIAMA. NSFC (#61075051) is acknowledged by BG Hu.

Appendix A. Derivation of the gradient calculation formula

Evaluating the scalar product $\sum_{n=0}^{N}[\overline{\mathbf{x}}_n]^{\mathrm{T}}\widehat{\mathbf{x}}_n$ in space $\underbrace{\mathbb{R}^m \times \cdots \times \mathbb{R}^m}_{N+1}$ by applying tangent linear model (18), we have

$$\sum_{n=0}^{N}[\overline{\mathbf{x}}_n]^{\mathrm{T}}\widehat{\mathbf{x}}_n = [\overline{\mathbf{x}}_0]^{\mathrm{T}}\widehat{\mathbf{x}}_0 + \sum_{n=0}^{N-1}[\overline{\mathbf{x}}_{n+1}]^{\mathrm{T}}\left[\frac{\partial F}{\partial \mathbf{x}}(\mathbf{x}_n, U_n)\widehat{\mathbf{x}}_n + \frac{\partial F}{\partial U}(\mathbf{x}_n, U_n)\widehat{U}_n\right] = [\overline{\mathbf{x}}_0]^{\mathrm{T}}\widehat{\mathbf{x}}_0$$
$$+ \sum_{n=0}^{N-1}\left\{\left[\left[\frac{\partial F}{\partial \mathbf{x}}(\mathbf{x}_n, U_n)\right]^{\mathrm{T}}\overline{\mathbf{x}}_{n+1}\right]^{\mathrm{T}}\widehat{\mathbf{x}}_n\right\} + \sum_{n=0}^{N-1}\left\{\left[\left[\frac{\partial F}{\partial U}(\mathbf{x}_n, U_n)\right]^{\mathrm{T}}\overline{\mathbf{x}}_{n+1}\right]^{\mathrm{T}}\widehat{U}_n\right\}. \tag{A.1}$$

This equals to:

$$[\overline{\mathbf{x}}_N]^{\mathrm{T}}\widehat{\mathbf{x}}_N + \sum_{n=0}^{N-1}[\overline{\mathbf{x}}_n]^{\mathrm{T}}\widehat{\mathbf{x}}_n = [\overline{\mathbf{x}}_0]^{\mathrm{T}}\widehat{\mathbf{x}}_0 + \sum_{n=0}^{N-1}\left\{\left[\left[\frac{\partial F}{\partial \mathbf{x}}(\mathbf{x}_n, U_n)\right]^{\mathrm{T}}\overline{\mathbf{x}}_{n+1}\right]^{\mathrm{T}}\widehat{\mathbf{x}}_n\right\}$$
$$+ \sum_{n=0}^{N-1}\left\{\left[\left[\frac{\partial F}{\partial U}(\mathbf{x}_n, U_n)\right]^{\mathrm{T}}\overline{\mathbf{x}}_{n+1}\right]^{\mathrm{T}}\widehat{U}_n\right\} + \sum_{n=0}^{N-1}\left\{\left[\frac{\partial l}{\partial \mathbf{x}}(\mathbf{x}_n, U_n)\right]\widehat{\mathbf{x}}_n\right\} - \sum_{n=0}^{N-1}\left\{\left[\frac{\partial l}{\partial \mathbf{x}}(\mathbf{x}_n, U_n)\right]\widehat{\mathbf{x}}_n\right\}. \tag{A.2}$$

Recall that in tangent linear model (18) and adjoint model (20), $\overline{\mathbf{x}}_N = 0$, and $\widehat{\mathbf{x}}_0 = 0$, arranging the items in (A.2) we have

$$\sum_{n=0}^{N-1}\left\{\left[\frac{\partial l}{\partial \mathbf{x}}(\mathbf{x}_n, U_n)\right]\widehat{\mathbf{x}}_n\right\} = \sum_{n=0}^{N-1}\left[-\overline{\mathbf{x}}_n + \left[\frac{\partial F}{\partial \mathbf{x}}(\mathbf{x}_n, U_n)\right]^{\mathrm{T}}\overline{\mathbf{x}}_{n+1} + \left[\frac{\partial l}{\partial \mathbf{x}}(\mathbf{x}_n, U_n)\right]^{\mathrm{T}}\right]^{\mathrm{T}}\widehat{\mathbf{x}}_n$$
$$+ \sum_{n=0}^{N-1}\left\{\left[\left[\frac{\partial F}{\partial U}(\mathbf{x}_n, U_n)\right]^{\mathrm{T}}\overline{\mathbf{x}}_{n+1}\right]^{\mathrm{T}}\widehat{U}_n\right\}. \tag{A.3}$$

Recall the definition of the adjoint model (20), we get

$$\sum_{n=0}^{N-1}\left\{\left[\frac{\partial l}{\partial \mathbf{x}}(\mathbf{x}_n, U_n)\right]\widehat{\mathbf{x}}_n\right\} = \sum_{n=0}^{N-1}\left\{\left[\left[\frac{\partial F}{\partial U}(\mathbf{x}_n, U_n)\right]^{\mathrm{T}}\overline{\mathbf{x}}_{n+1}\right]^{\mathrm{T}}\widehat{U}_n\right\}. \tag{A.4}$$

The first-order variation $\widehat{\mathcal{J}}$ resulting from the perturbation $\widehat{\mathbf{U}}$ can be evaluated by the directional derivative which is the projection of the gradient on the chosen direction $\widehat{\mathbf{U}}$. Substitute (A.4) into (19), and let $\langle\,\rangle$ be the inner product in Euclidean space $\mathbb{R}^N$, we have

$$\widehat{\mathcal{J}} = \langle \nabla\mathcal{J}, \widehat{\mathbf{U}}\rangle = \sum_{n=0}^{N-1}\left\{\left[\left[\frac{\partial F}{\partial U}(\mathbf{x}_n, U_n)\right]^{\mathrm{T}}\overline{\mathbf{x}}_{n+1}\right]^{\mathrm{T}}\widehat{U}_n\right\} + \sum_{n=0}^{N-1}\left(\frac{\partial l}{\partial U}(\mathbf{x}_n, U_n)\widehat{U}_n\right)$$
$$= \sum_{n=0}^{N-1}\left\{\left\{\left[\left[\frac{\partial F}{\partial U}(\mathbf{x}_n, U_n)\right]^{\mathrm{T}}\overline{\mathbf{x}}_{n+1}\right]^{\mathrm{T}} + \frac{\partial l}{\partial U}(\mathbf{x}_n, U_n)\right\}\widehat{U}_n\right\}$$
$$= \left\langle \begin{bmatrix} \left[\frac{\partial F}{\partial U}(\mathbf{x}_0, U_0)\right]^{\mathrm{T}}\overline{\mathbf{x}}_1 + \left[\frac{\partial l}{\partial U}(\mathbf{x}_0, U_0)\right]^{\mathrm{T}} \\ \vdots \\ \left[\frac{\partial F}{\partial U}(\mathbf{x}_{N-1}, U_{N-1})\right]^{\mathrm{T}}\overline{\mathbf{x}}_N + \left[\frac{\partial l}{\partial U}(\mathbf{x}_{N-1}, U_{N-1})\right]^{\mathrm{T}} \end{bmatrix}, \begin{bmatrix} \widehat{U}_0 \\ \vdots \\ \widehat{U}_{N-1} \end{bmatrix}\right\rangle. \tag{A.5}$$

Therefore the gradient $\nabla\mathcal{J}$ can be calculated as formula (21).

References

[1] C. Bardos, O. Pironneau, Data assimilation for conservation laws, Methods Appl. Anal. 12 (2005) 103–134.
[2] P. Boggs, J. Tolle, Sequential quadratic programming, Acta Numer. 4 (1995) 1–51.
[3] J.F. Bonnans, J.C. Gilbert, C. Lemarechal, C.A. Sagastizábal, Numerical Optimization: Theoretical and Practical Aspects, second edition, Springer, 2006.
[4] C. Brouwer, H. Heibloem, Irrigation Water Management, Training Manuals – 3: Irrigation Water Needs, Food and Agriculture Organization of the United Nations, 1986.
[5] W. Chao, L.P. Chang, Development of a four-dimensional variational analysis system using the adjoint method at GLA. Part 1. Dynamics, Mon. Weather Rev. 120 (1992) 1661–1673.
[6] M. Chelle, Phylloclimate or the climate perceived by individual plant organs: What is it? how to model it? What for? New Phytol. 166 (2005) 781–790.
[7] P.H. Cournède, M. Kang, A. Mathieu, J.F. Barczi, H. Yan, B.G. Hu, P. de Reffye, Structural factorization of plants to compute their functional and architectural growth, Simul. Trans. Soc. Modell. Simul. Int. 82 (2006) 427–438.
[8] E. Dayan, E. Presnov, M. Fuchs, Prediction and calculation of morphological characteristics and distribution of assimilates in the Rosgro model, Math. Comput. Simul. 65 (2004) 101–116.
[9] R. Giering, T. Kaminski, Recipes for adjoint code construction, ACM Trans. Math. Software 24 (1998) 437–474.
[10] P. Gill, W. Murray, M. Wright, Practical Optimization, Academy Press, 1981.
[11] A. Griewank, Evaluating Derivatives: Principles and Techniques of Algorithmic Differentiation, SIAM, Philadelphia, PA, 2000.
[12] Y. Guo, Y. Ma, Z. Zhan, B. Li, M. Dingkuhn, D. Luquet, P. de Reffye, Parameter optimization and field validation of the functional structural model GREENLAB for maize, Ann. Bot. 97 (2006) 217–230.
[13] Y. Guo, P. de Reffye, Y.H. Song, Z.G. Zhan, M. Dingkuhn, B. Li, Modeling of biomass acquisition and partitioning in the architecture of sunflower, in: B.G. Hu, M. Jaeger (Eds.), Plant Growth Modeling and Applications: Proceedings – PMA03, Tsinghua University Press and Springer, Beijing, 2003, pp. 271–284.
[14] F. Hallé, R. Oldeman, P. Tomlinson, Tropical Trees and Forests, Springer Verlag, Berlin, 1978.
[15] T.J. Howell, J.T. Musick, Relationship of dry matter production of field crops to water consumption, in: A. Perrier, C. Riou (Eds.), Proceedings of the International Conference Les Besoins en Eau des Cultures, INRA, Paris, 1985, pp. 247–269.
[16] M. Kang, P.H. Cournède, P. de Reffye, D. Auclair, B.G. Hu, Analytical study of a stochastic plant growth model: application to the GreenLab model, Math. Comput. Simul. 78 (2008) 57–75.
[17] W. Kurth, B. Sloboda, Growth grammars simulating trees—an extension of L-systems incorporating local variables and sensitivity, Silva Fenn. 31 (1997) 285–295.
[18] F.X. Le Dimet, H. Ngodock, B. Luong, J. Verron, Sensitivity analysis in variational data assimilation, J. Meteorol. Soc. Jpn. 75 (1997) 245–255.
[19] F.X. Le Dimet, O. Talagrand, Variational assimilation of meteorological observations: theoretical aspect, Tellus 38A (1986) 97–110.
[20] V. Letort, P. Mahe, P.H. Cournède, P. de Reffye, B. Courtois, Quantitative genetics and functional–structural plant growth models: simulation of quantitative trait loci detection for model parameters and application to potential yield optimization, Ann. Bot. 101 (2008) 1243–1254.
[21] J.L. Lions, Contrôle optimal de sysémes gouvernés par des équations aux dérivées partielles, Dunod: Gauthier-Villars, Paris, 1968.
[22] Y. Ma, B. Li, Z. Zhan, Y. Guo, D. Luquet, P. de Reffye, M. Dingkuhn, Parameter stability of the functional–structural plant model GREENLAB as affected by variation within populations, among seasons and among growth stages, Ann. Bot. 99 (2007) 61–73.
[23] J.C. Mailhol, A.A. Olufayo, P. Ruelle, Sorghum and sunflower evapotranspiration and yield from simulated leaf area index, Agric. Water Manage. 35 (1997) 167–182.
[24] L. Marcelis, E. Heuvelink, J. Goudriaan, Modelling biomass production and yield of horticultural crops: a review, Sci. Hortic. (Amsterdam) (1998) 83–111.
[25] A. Mathieu, P.H. Cournède, D. Barthélémy, P. de Reffye, Rhythms and alternating patterns in plants as emergent properties of a model of interaction between development and functioning, Ann. Bot. 101 (2008) 1233–1242.
[26] R. Mech, P. Prusinkiewicz, Visual models of plants interacting with their environment, Comput. Graph. 30 (1996) 397–410.
[27] J. Perttunen, R. Sievänen, E. Nikinmaa, H. Salminen, H. Saarenmaa, J. Väkevä, LIGNUM: a tree model based on simple structural units, Ann. Bot. 77 (1996) 87–98.
[28] P. Prusinkiewicz, Modeling plant growth and development, Curr. Opin. Plant Biol. 7 (2004) 79–83.
[29] R. Qi, V. Letort, M. Kang, P.H. Cournède, P. de Reffye, T. Fourcaud, Application of the GreenLab model to simulate and optimize wood production and tree stability: a theoretical study, Silva Fenn. 43 (2009) 465–487.
[30] F. Rabier, H. Järvinen, E. Klinker, J.F. Mahfouf, A. Simmons, The ECMWF operational implementation of four-dimensional variational assimilation. I. Experimental results with simplified physics, Quart. J. Roy. Meteorol. Soc. 126 (2000) 1143–1170.
[31] P. de Reffye, F. Blaise, S. Chemouny, S. Jaffuel, T. Fourcaud, F. Houllier, Calibration of a hydraulic architecture-based growth model of cotton plants, Agronomie 19 (1999) 265–280.
[32] P. de Reffye, C. Edelin, J. Françon, M. Jaeger, C. Puech, Plant models faithful to botanical structure and development, Comput. Graph. 22 (1988) 151–158.
[33] P. de Reffye, T. Fourcaud, F. Blaise, D. Barthélémy, F. Houllier, A functional model of tree growth and tree architecture, Silva Fenn. 31 (1997) 297–311.

[34] R. Sievänen, E. Nikinmaa, P. Nygren, H. Ozier-Lafontaine, J. Perttunen, H. Hakula, Components of a functional–structural tree model, Ann. For. Sci. 57 (2000) 399–412.
[35] O. Talagrand, The use of adjoint equations in numerical modelling of the atmospheric circulation, in: A. Griewank, G. Corliss (Eds.), Automatic Differentiation of Algorithms: Theory, Implementation, and Application, SIAM, 1991, pp. 169–180.
[36] L. Wu, Variational methods applied to plant functional–structural dynamics: parameter identification, control, and data assimilation, Ph.D. thesis, Université Joseph Fourier, 2005.
[37] L. Wu, V. Mallet, M. Bocquet, B. Sportisse, A comparison study of data assimilation algorithms for ozone forecasts, J. Geophys. Res. 113 (2008) D20310.
[38] L. Wu, P. de Reffye, B.G. Hu, F.X. Le Dimet, P.H. Cournède, A water supply optimization problem for plant growth based on GreenLab model, J. ARIMA (2005) 194–207.
[39] H. Yan, M. Kang, P. de Reffye, M. Dingkuhn, A dynamic, architectural plant model simulating resource dependent growth, Ann. Bot. 93 (2004) 591–602.
[40] Z. Zhan, P. de Reffye, F. Houllier, B.G. Hu, Fitting a functional–structural growth model to plant architecture data, in: B.G. Hu, M. Jaeger (Eds.), Plant Growth Modeling and Applications: Proceedings – PMA03, Tsinghua University Press and Springer, Beijing, 2003, pp. 236–249.
[41] J. Zhu, M. Kamachi, G. Zhou, Nonsmooth optimization approaches to VDA of models with on/off parameterizations: Theoretical issues, Adv. Atmos. Sci. 19 (2002) 405–424.
[42] X. Zou, F. Vandenberghe, M. Pondeca, Y.H. Kuo, Introduction to adjoint techniques and the MM5 adjoint modeling system, Technical Report, NCAR, 1997.
[43] B.G. Hu, P. de Reffye, X. Zhao, H.P. Yan, M.Z. Kang, GreenLab: A new methodology towards plant functional-structual model-Structual aspect, in: B.G. Hu, M. Jaeger (Eds.), Plant Growth Modeling and Applications: Proceedings – PMA03, Tsinghua University Press and Springer, Beijing, 2003, pp. 21–35.